IEEE Journal of Microwaves

Received 14 December 2021; revised 7 March 2022 and 22 April 2022; accepted 16 May 2022. Date of publication 9 June 2022; date of current version 7 July 2022.

Digital Object Identifier 10.1109/JMW.2022.3177578

A Two-Stage Wideband RF Cancellation of Coupled Transmit Signal for Bi-Static Simultaneous Transmit and Receive System

MD NURUL ANWAR TAREK [1] (Graduate Student Member, IEEE), RIMON HOKAYEM [2] (Member, IEEE), SANDHIYA REDDY GOVINDARAJULU [3] (Student Member, IEEE), MARKUS H. NOVAK [3] (Member, IEEE), AND ELIAS A. ALWAN [1] (Member, IEEE)

(Regular Paper)

[1]Department of Electrical Engineering, Florida International University, Miami, FL 33174 USA
[2]Silicon Labs, Montreal, QC H3B 4C9, Canada
[3]Novaa Limited, Columbus, OH 43210 USA

CORRESPONDING AUTHOR: Md Nurul Anwar Tarek (e-mail: mtare002@fiu.edu).

This work was supported in part by Novaa Ltd., U.S. Army Research Laboratory and Army SBIR Program Office under Grant W911QX-18-P-0186, and in part by NSF under Grant 1943040.

ABSTRACT Wireless technology is growing at a fast rate to accommodate the expanding user demands. Currently, the radio frequency (RF) spectrum is overcrowded. Hence, it is more susceptible to signal fratricide and interference. To enhance spectrum access, in-band full duplex systems are implemented to achieve simultaneous transmission and reception (STAR) and double the spectral efficiency. However, STAR systems require suppression of the high power transmit signals that can leak into the receiver chain. This type of self-interference (SI) can significantly reduce the receiver.s dynamic range and often leads to its desensitization. Therefore, successful STAR implementation requires considerable isolation between the transmitter and receiver to reduce the SI signal. To do so, RF self-interference cancellation (RFSIC) stages are considered. In this paper, we present a two-stage SIC system that includes transmit and receive antennas isolation and RFSIC filter stages. Notably, the isolation between the transmit and receive antennas is based on a novel symmetric suppression technique. The RFSIC filter is based on a hybrid finite impulse response (FIR) filter and resonator architecture. Adding a resonator to the FIR filter provides improved matching to approximate and suppress the direct SI coupling. Our design achieves ∼52 dB isolation on average across a 500 MHz bandwidth (*viz.* 1-1.5 GHz) in simulation. Simulation results show a minimum cancellation of 41 dB and a maximum cancellation of 65 dB. A prototype was fabricated and tested, showing an average of ∼ 44 dB cancellation which is in good agreement with our simulation.

INDEX TERMS Coupling signal, in-band full duplex (IBFD), STAR, self-interference cancellation (SIC).

I. INTRODUCTION

Current electromagnetic spectrum (EM) is too congested to facilitate a continuous frequency spectrum for ultra-wideband (UWB) communication [1]–[4]. This limitation has spurred the necessity for efficient spectrum access techniques such as in-band full-duplex (IBFD) or simultaneous transmit and receive (STAR) [5]–[7]. The latter enables a cellular network to transmit and receive simultaneously over the same frequency band [8]. As such, STAR enables frequency re-use. Hence, the spectral efficiency is doubled. Since the existing RF spectrum is very costly, greater spectrum efficiency in the STAR system implies significant cost reduction for spectrum licensing [9].

The key challenge to realize STAR systems is in mitigating self-interference (SI) [10], [11]. The latter refers to the high power transmit signal that couples to the receiver port, which is typically ∼ 100 dB stronger than the received signal, and causes receiver desensitization [2]. To circumvent this issue, typical communication systems have adopted different

methods such as time-division duplexing (TDD) or frequency division duplexing (FDD) [4], [12]–[15]. However, these duplexing schemes exploit orthogonality of time/frequency resources at the expense of spectral efficiency [16]. In brief, TDD and FDD occupy double the time and frequency, respectively. In addition, TDD requires stringent time/phase synchronization to realize full-duplex, whereas FDD uses extra guard band beyond its dedicated transmit (Tx)/Receive (Rx) frequencies.

Alternatively, doubling the spectral efficiency can be achieved using STAR systems [17]. The successful implementation of these systems requires high isolation between transmitter and receiver of as much as 100 dB [17]–[22]. To do so, we must 1) cancel the transmit signals that directly couple to the receiver chain, 2) suppress harmonics from power amplifiers (PAs), and 3) eliminate coupled noise from the Tx chain. Further, advanced STAR circuits are needed to remove multipath reflected signals. Notably, coupled interference suppression from nearby transmitters should be enacted adaptively to unlock the impact of dynamically varying environments.

So far, STAR implementations have overcome the unwanted SI through the implementation of multiple stages of coupled signal suppression techniques across the receiver chain. As such, SI cancellation was achieved in 1) propagation domain, 2) analog domain, and 3) digital domain [23]. Propagation domain cancellation was accomplished by employing techniques such as cross-polarization of Tx/Rx antenna or Tx beamforming [24]–[27]. Notably, these techniques have shown that SI becomes even higher in the case of an antenna array. Therefore, to realize an efficient STAR system, the interfering signal must be sufficiently cancelled at subsequent RF and baseband stages. Analog stage cancellation incorporates an RF filter to cancel the replica of the transmit signal from the receiver chain [16], [28], [29]. However, analog self-interference cancellation (SIC) needs to achieve enough cancellation to preserve the analog to digital converter (ADC) dynamic range (DR). For a linear ADC, the DR is calculated using DR=6.02n +1.76 (dB) [30]. Hence, assuming a 12 b ADC (including a 2 b margin), the dynamic range is 62 dB. Therefore, we require 48 dB of analog suppression to achieve a total of 110 dB cancellation. The digital domain involves probabilistic modeling of the propagation channel for post-processing the digitized signal to further reduce the SI in the receiver chain [31].

However, most of these STAR topologies have only been applied to narrow band signals (*viz.* <100 MHz) [32]–[35]. Frequency selectivity at the antenna interface limits the SIC bandwidth. Conventional RF canceller mimics at a single frequency point, limiting the SIC bandwidth to achieve infinite cancellation. For wideband SIC cancellation, we need to mimics the SI signal at several frequencies to extend the SIC bandwidth. In a recent work [34], an RF front-end for a full duplex radio system with three antennas (ATRX1, ATRX2, and ARXD) is presented. The transmitting signal is first fed to a rat race coupler with two output transmit antennas (ATRX1 and ATRX2). The transmit signals at ATRX1 and ATRX2 are summed out of phase at the differential port of the rat race coupler and fed to the receive antenna port (ARXD). At the receiver side, two SI reference generators are implemented to further reduce the residual signal by 60 dB across 80 MHz. In our work, one TX and 2 RX antennas were employed with 1 splitter, 2 directional couplers, 1 hybrid coupler, and 2 custom-made SIC FIR resonator. Our design achieves 52 dB across 500 MHz. Furthermore, in our work, we are using direct coupling in the RF domain instead of residual signals in the time domain used in [34]. We note that direct coupling provides more cancellation across a wider bandwidth. In [35], two narrow band tunable resonators were used in the antenna array near field to provide a 30 dB reduction in Tx/Rx coupling across 110 MHz.

Recently, researchers have been working on fully integrated RFIC incorporating SIC for STAR system. In [36], a multiple-stage bandpass filter (BPF) is implemented using nanoscale CMOS technology for SI cancellation in the RF domain. Tunability, reconfigurability, and high Q are the favorable features for this CMOS implementation. However, this technique is capable of achieving 20 dB of SIC across a 20 MHz bandwidth (BW). A CMOS transceiver is implemented with 65 dB deep Tx SI cancellation across 80 MHz in another study [37]. In [38], a seven-tap RF canceller with time-interleaved switched capacitor delays is designed in a 65 nm CMOS platform. However, this technique can operate in narrow BW and provides an average of 32.5 dB cancellation across 20 MHz BW.

Multi-tap finite impulse response (FIR) filters were also implemented for SIC. Particularly, a 16-tap filter was implemented in [18] and demonstrated 47 dB cancellation across a narrow bandwidth of 80 MHz. This cancellation circuit used a large number of attenuators (in this case, 16) implying additional complexity of the optimization algorithm that was used. In [39], a time-domain narrowband cancellation using a filter with four tap delay lines and attenuators demonstrated 30 dB cancellation across a BW of 30 MHz. Researchers in [40] used multiple RF bandpass filters to implement RF-SIC in the canceller that channelizes the desired bandwidth. This approach showed 20 dB of SI cancellation across 27 MHz. Other multi-stage STAR implementations introduced a stage of digital baseband cancellations to achieve up to 60-80 dB cancellation [41], [42].

More recently, research on wideband STAR systems abound. In [43], one pair of Tx and one pair of Rx antennas were designed with two 3 dB 180° hybrid couplers, resulting in 39.6 dB of SI cancellation across 4:1 BW. Another study showed 35 dB Tx/Rx isolation across 2-2.9 GHz using a ring array [44]. However, this approach requires an external beamformer to improve isolation to 50 dB, implying additional complexity (see Table 1 in Section VIII). In [3], [16], wideband FIR filters were implemented to provide RF cancellation across 500 MHz. Indeed, multi-tap FIR filter provides more degrees of freedom (such as tunability and attenuation) to achieve cancellation across larger bandwidth. This approach was able to achieve 25 dB RF cancellation across 500 MHz.

TABLE 1. Performance Comparison With the State-of-the-Art in STAR System Implementations

Band	Reference	Bandwidth	TX-RX isolation	Technology	Stages
Narrowband	[35]	80 MHz	60 dB	3 antennas (2 Tx and 1 Rx), SI signal generator	Three stages
Narrowband	[36]	110 MHz	30 dB	Near-field filter	Two stages
Narrowband	[37]	20 MHz	20 dB	Bank of band pass filter	RF stage
Narrowband	[38]	80 MHz	65 dB	Double RF canceller	Three stages
Narrowband	[39]	20 MHz	32.5 dB	RF canceller and BB canceller	Two stages
Narrowband	[40]	20 MHz	78 dB	Multi–tap RF canceller	Two stages
Narrowband	[41]	27 MHz	20 dB	Multiple RF band pass filter	Two stages
Narrowband	[42]	5 MHz	60 dB	2 Tx and 1 Rx, QHx220 chip, digital cancellation	Three stages
Narrowband	[43]	10 MHz	73dB	Signal inversion, digital cancellation	Three stages
Wideband	[28]	500 MHz	25 dB	FIR filter	Only RF stage is shown
Wideband	[44]	4:1 BW	39.5 dB	Spiral antenna, hybrid (But it is mo-static STAR system)	Two stages
Wideband	[45]	900 MHz	35 dB	8 Tx and 1 Rx, mutual coupling suppression	Single stage
			50 dB	8 Tx and 1 Rx, added external beamformer	Two stages
Wideband	[47]	1 GHz	25 dB	FIR filter bank	Only RF stage is shown
Wideband	**This work**	**500 MHz**	**52 dB (sim.)**	**1 Tx and 2 Rx, 2 SIC circuits, symmetric SI suppression**	**Two stages**
			44 dB (meas.)		

This work was later expanded to obtain 25 dB cancellation across 1 GHz bandwidth by cascading multiple FIR filters [45], [46]. However, this cascaded approach is hardware intensive.

In this paper, we present a two-stage wideband STAR architecture operating across 500 MHz, as shown in Fig. 1. This is an extension of our previous work, published in [47], that was solely based on simulation. This paper brings forward several novelties, among them:

1) The passive symmetric cancellation technique is introduced in the RF domain and is achieved using two customized SIC circuits.
2) The SIC circuit is novel and based on a hybrid FIR filter and resonator topology. The resonator adds extra flexibility to approximate the SI signal.
3) The cancellation is 30 dB across a wide bandwidth of 500 MHz. Other published work showed 30 dB cancellation across 80 MHz [34].
4) The benefit of passive symmetric RF cancellation is that we can achieve additional SIC cancellation using a 180-degree hybrid coupler,
5) Since implementing the FIR resonator requires a high tuned solution and no initial guess, we have chosen a differential evolution (DE) algorithm. DE is a population-based optimizer for finding the best solution of a problem. DE, in its most basic form, is the process of adding the weighted difference between two population vectors to a third vector. The differential evolution algorithm works well for no initial solution and is also effective for a high-tuned solution.

Our STAR architecture was able to achieve 41 dB minimum to 65 dB maximum isolation (simulation) and 40 dB minimum to 50 dB maximum isolation (measurement) between the Tx and the two Rx ports across 1 to 1.5 GHz. In particular, we introduce a symmetric coupling suppression technique using a three-element antenna array. The symmetry between the Tx and each of the Rx antennas leads to a of 12 dB isolation. The latter can potentially improve to 32.5 dB if a 180° hybrid coupler is used to combine the two Rx ports. Instead, more isolation can be achieved by introducing an RF stage using a novel six-tap FIR-resonator circuit between Tx and Rx antenna. This achieves a total cancellation of 40 dB. Finally, the 180° hybrid is employed between the Rx ports to further improve on average cancellation down to 52 dB.

Overall, the proposed architecture improved spectral efficiency across various space communication bands including L band by providing highly coveted isolation of 52-70 dB. We anticipate that the triad of antenna isolation, customized SIC filters suppression, and couplers will lead the way for practical, secure, and spectrally efficient STAR radios for space and satellite communication. It is noted that STAR technology also provides great advantages for magnetic resonance imaging (MRI) where a significant amount of isolation is the crucial requirement over various loading conditions in an MRI scanner [48]. In summary, the applications include next-generation (5 G/6 G) wireless systems, phased array radar systems, military, law enforcement, and aerospace communications, pulse-Doppler radar systems, biomedical field, etc.

This paper is structured as follows. Section II describes the principle of the operation of the symmetric SIC technique. In Section III, we show symmetric coupling suppression using the three antenna structure and 3-dB hybrid coupler. In Section IV, we perform symmetric coupling suppression using our novel SIC circuits. Section V shows the simulation

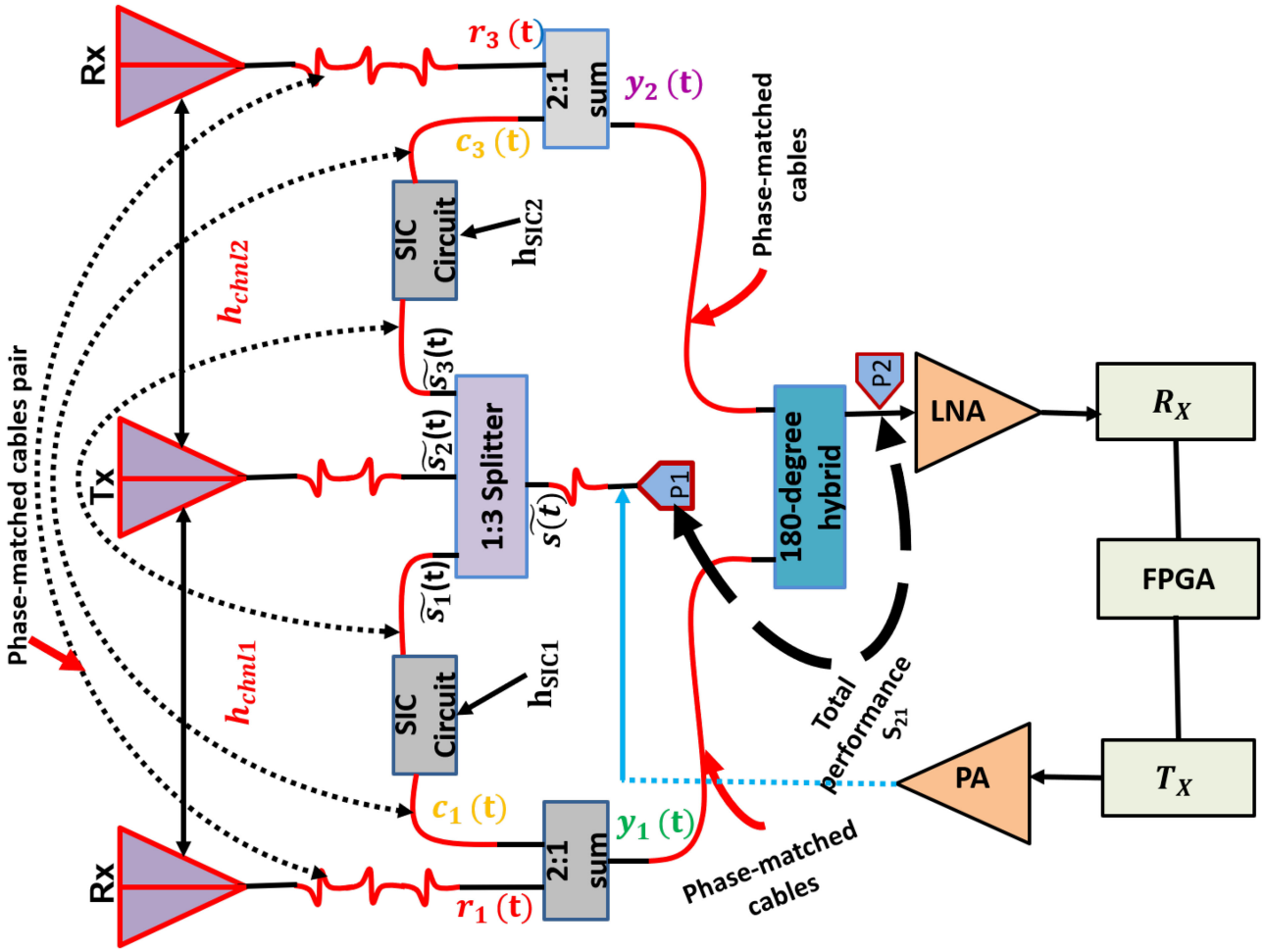

FIGURE 1. A two-stage wideband STAR system operating across 500 MHz. The architecture is based on symmetric coupling suppression at the antenna stage, followed by two SIC circuits, and a hybrid coupler. The total SIC is up to 52 dB.

performance of the SIC circuit. Sections VI and Section VII show the fabricated prototype and measurement setup, respectively. Section VIII presents a comparison of our system with other state-of-the-art STAR implementations. Section IX concludes the paper.

II. A TWO-STAGE RF SELF -INTERFERENCE CANCELLATION

In this paper, a compact, symmetric, analog RF cancellation is developed across a wide bandwidth, *viz.* 500 MHz. The whole architecture consists of a three-element antenna array, one for Tx and two for Rx, two SIC circuits, three power splitters, and one power combiner, as depicted in Fig. 1. In bistatic STAR, one pair of Tx and Rx antennas is common in practice to achieve a balanced configuration and provide sufficient SIC cancellation. The design of the entire system is presented first, followed by a detailed procedure of the RF SIC circuits design and optimization from 1 to 1.5 GHz.

As already mentioned, STAR systems require significant cancellation of the coupled Tx signal into the Rx chains. Coupling suppression can be achieved by improving the isolation between the Tx and Rx antennas, as well as introducing SIC circuits at the RF and/or analog/digital baseband. In our design, two Rx antennas are placed at equal distance away from the Tx antenna, as shown in Fig. 2(a).

A prototype was fabricated, as shown in Fig. 2(b). The isolation between the Tx and each of the Rx antennas is 12 dB. Notably, the coupled signals at each Rx antenna are symmetric and fed to a 180° hybrid coupler to achieve >32.5 dB coupling suppression at the antenna stage, as shown in Fig. 2(c). The antenna isolation alone is not enough for STAR implementation, as for high Tx power (on the order of a few dBW), the coupled signal after the antenna stage is still very high and risks to desensitize the Rx chain. Therefore, an additional stage is introduced to further improve on average cancellation down to 52 dB. An SIC circuit is implemented between the Tx antenna and each of the Rx antennas (see Fig. 1). The SIC circuits are designed with a response conjugately matched to the coupling between the Tx and each of the Rx antennas. To do so, a 3-way power splitter is used to split the transmit signal. One output is fed to the Tx antenna. The other two

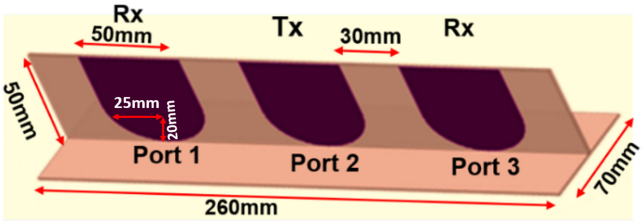

(a)

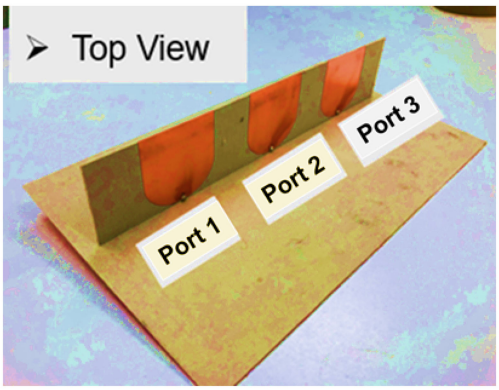

(b)

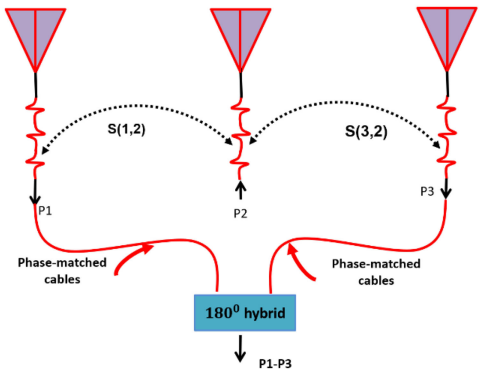

(c)

FIGURE 2. (a) Simulated 3 element monopole array; (b) Fabricated prototype of 3 element monopole array; and (c) Schematic of a SIC for 3 element monopole array using hybrid coupler.

outputs are fed to each of the SIC circuits between the Tx and Rx ports.

At each of the Rx chains, the SIC circuit's output is combined with the coupled signal using a power combiner to achieve the required cancellation. The combiner's output is then fed to an 180° hybrid coupler to cancel out the total coupling at both antenna elements. This approach demonstrates better symmetric cancellation in the RF stage. Finally, the output of the hybrid coupler is fed to the Rx chain. Also note that the SIC circuits are implemented between the Tx and Rx chains and not along the Rx chains. Therefore, these circuits will not affect neither the Tx neither the Rx signals, and will not contribute to any additional losses. However, there is a loss of 4.77 dB at the TX port. But at the same time, with

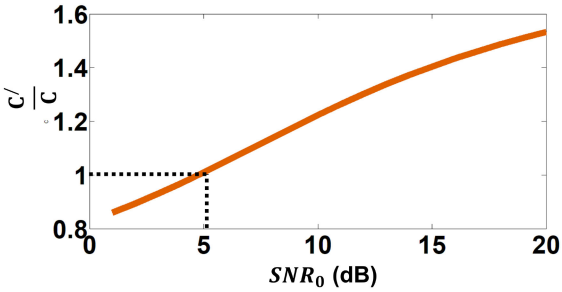

FIGURE 3. Channel capacity ratio between FD and traditional system.

this loss, we were able to feed the two SIC filters. Previous work [37] has used only one SIC. In this case, a power splitter with a loss of 3 dB is needed. However, only a single SIC was used and a cancellation of 65 dB was achieved across 80 MHz. Conversely, in this work, using a 3-way power splitter, we could achieve a minimum of 41 dB and a maximum of 65 dB cancellation across 500 MHz with a loss of only 4.77 dB.

It is worth mentioning that such a loss does not greatly affect the Full Duplex (FD) capacity. This can be validated by referring to the basic transceiver's channel capacity, specified as $C{=}BW.log_2(1+10^{\frac{SNR_0}{10}})$. Here, BW denotes the channel bandwidth and SNR_0 denotes the received signal-to-noise ratio. In our FD system, the bandwidth BW increases to 2BW, however with an SNR_0 reduction of 4.77 dB due to 4.77-dB losses in both Tx and Rx chains. As a result, the new channel capacity is equal to $C^{/} = 2B.log_2(1+10^{\frac{SNR_0-4.77}{10}})$ To achieve a higher capacity (*viz.* $C^{/}C \geq 1$) with our system, SNR_0 5.01 dB is needed, as shown in Fig. 3. We note that most digital modulations schemes require a minimum SNR_0 of 10 to 15 dB which imply that our system will always achieve a high capacity that traditional systems.

More details on the antenna design and SIC circuits are provided in the next section.

III. ANTENNA ISOLATION

For symmetric coupling cancellation, the geometry of the linear 3-element monopole antenna array is shown in Fig. 2(a). The total antenna dimensions (L × W×h) are 260 mm×70 mm×50 mm. Fig. 2(a) shows that the geometry of the designed monopole array consists of rectangular patch with width=50 mm, length=50 mm, and an elliptical patch of radius ratio equal to 1.25 with major axis equal to 25 mm, and minor axis equal to 20 mm. The addition of elliptical patch improves the bandwidth of the monopole antenna array. The Tx antenna (Port 2) is placed at the center of the array. The two Rx antennas (Port 1 and Port 3) are placed at equal distance away from the center element (*viz.* 80 mm). The prototype (see Fig. 2(b)) is printed on a Rogers 5880 substrate with loss tangent of 0.0009, dielectric constant of 2.2, and a substrate thickness of 1.27 mm. To achieve high isolation between the Tx antenna and both Rx antennas, the transmission coefficients S(1,2) and S(3,2) are required to be identical. This is realized using a perfectly symmetric configuration. As

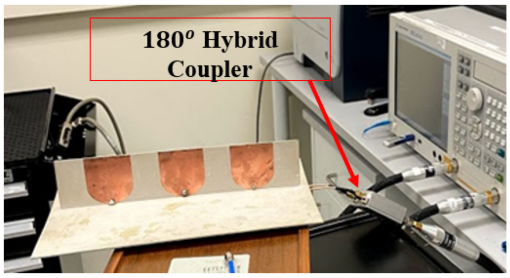

FIGURE 4. Photograph of a SIC setup for fabricated 3 element monopole array using hybrid coupler.

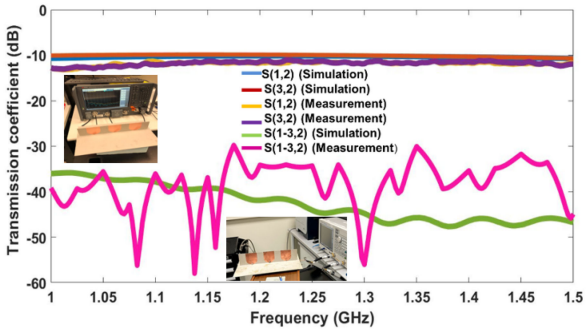

FIGURE 5. Transmission coefficient at different ports. Coupling channels from Tx to Rx antennas are nearly identical resulting in significant cancellation when combined (pink color) showing the measured isolation of 36 dB.

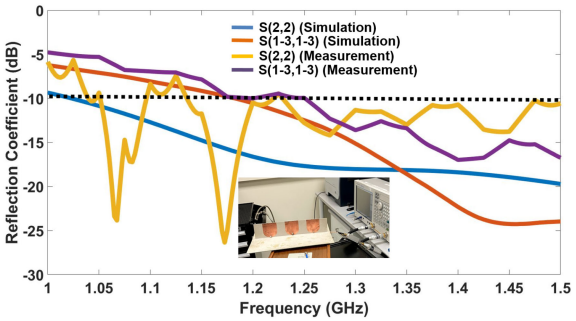

FIGURE 6. Simulation and measurement of the active reflection coefficient for the 3-element monopole array prototype.

such, the coupled signals at each of the Rx ports are identical. When combined out of phase using a 180° hybrid coupler (see Fig. 2(c)), the coupled Tx signal is substantially reduced. The 3-element antenna prototype with the hybrid coupler was tested, as shown in Fig. 4.

A ∼36 dB isolation was measured across 1–1.5 GHz band, as shown in Fig. 5. We note that, we have not designed the hybrid coupler. It was purchased from a vendor with ∼3.5 dB insertion loss. The part number for this item is ZAPDJ-2. Therefore, the actual antenna isolation without hybrid coupler insertion loss is ∼32.5 dB. Fig. 6 shows the simulated and measured reflection coefficients at each of the ports. The phase coupling and its corresponding antiphase response are also

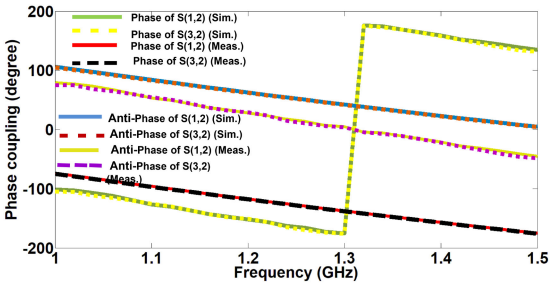

FIGURE 7. Simulation and measurement of phase and anti-phase response of symmetric coupling path between the Tx and each of the Rx antenna ports.

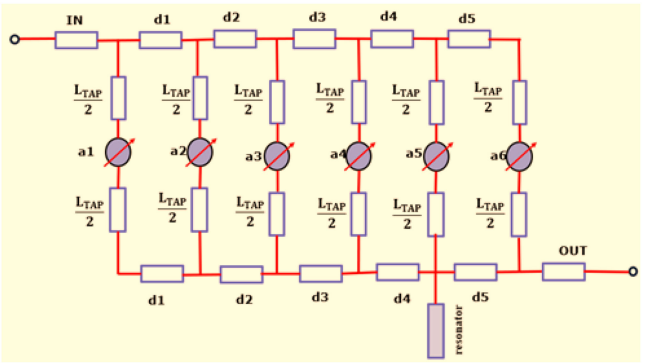

FIGURE 8. RF FIR-resonator circuit operating across 500 MHz. This circuit consists of delay lines, attenuators, and a resonator stub. The order of filter is determined by the number of taps.

shown in Fig. 7. The antiphase coupling is required to improve isolation, as will be discussed in the following section.

IV. SYMMETRIC COUPLING CANCELLATION IN THE RF STAGE

The symmetric configuration of the antennas demonstrates up to 32.5 dB of isolation. Additional suppression can be achieved (>50 dB) by employing a second stage of SIC at the RF front-end, as depicted in Fig. 1. The SIC circuit at the front-end is a hybrid combination of an FIR filter and a resonator, as depicted in Fig. 8. RF cancellation is achieved by tapping the transmitted signal prior to transmission, then applying gain/delay adjustments using SIC circuit, and subsequently inserting the modified signal into the Rx chain for cancellation. More in detail, the coupling between the Tx and each of the Rx antennas is represented by the impulse response h_{chnl1} and h_{chnl2} (see Fig. 1), respectively. Since both coupling are identical,

$$S(1,2) = S(2,3) \tag{1}$$

The scattering parameters are related to the channel impulse response using [1]:

$$h_{chnl1} = \frac{S(1,2)(1-\Gamma_L)(1-\Gamma_S)}{(1-S(1,1)\Gamma_L)(1-S(2,2)\Gamma_S) - S(2,1)\Gamma_L S(1,2)\Gamma_S} \tag{2}$$

$$h_{chnl2} = \frac{S(3,2)(1-\Gamma_L)(1-\Gamma_S)}{(1-S(3,3)\Gamma_L)(1-S(2,2)\Gamma_S)-S(2,3)\Gamma_L S(3,2)\Gamma_S} \quad (3)$$

where, Γ_L and Γ_S are the reflection at the source and load of the two-port network formed by the Tx and each of the Rx ports. Under matching condition, $\Gamma_L = \Gamma_S = S(1,1) = S(2,2) = S(3,3) = 0$

Hence, (2) and (3) become

$$h_{chnl1} = S(1,2) \quad (4)$$

$$h_{chnl2} = S(3,2) \quad (5)$$

Referring to (1)

$$h_{chnl1} = h_{chnl2} \quad (6)$$

In Fig. 1, we define $s(t)$ as the power amplifier's (PA) output signal and $\widetilde{s}_2(t)$ as the output of the power splitter feeding the Tx antenna port. $\widetilde{s}_1(t)$ and $\widetilde{s}_3(t)$ are the signals at ports 1 and 3 of the power splitter, that will be fed to the each of the SIC circuits, respectively. The coupled signals $\widetilde{r}_1(t)$ and $\widetilde{r}_3(t)$ represent the SI at ports 1 and 3 of the Rx antennas, respectively, such as

$$r_1(t) = \widetilde{s}_1(t) * h_{chnl1}(t) \quad (7)$$

$$r_3(t) = \widetilde{s}_3(t) * h_{chnl2}(t) \quad (8)$$

To cancel these coupled SI signals, the outputs of the power splitter $\widetilde{s}_1(t)$ and $\widetilde{s}_3(t)$ are passed through the two designed RF SIC circuits of impulse responses $h_{sic1}(t)$ and h_{sic2} (t), respectively. The filtered signals at each Rx ports are then,

$$c_1(t) = \widetilde{s}_1(t) * h_{sic1}(t) \quad (9)$$

$$c_3(t) = \widetilde{s}_3(t) * h_{sic2}(t) \quad (10)$$

At the Rx ports, a 2:1 power combiner is employed. The combined Rx signals from both symmetric sides are:

$$y_1(t) = c_1(t) + r_1(t) \quad (11)$$

$$y_2(t) = c_3(t) + r_3(t) \quad (12)$$

Thus, our goal is to minimize $y_1(t)$ and $y_2(t)$. This is accomplished by designing SIC circuits with the following impulse response:

$$h_{sic1}(t) = -h_{chnl1}(t) \quad (13)$$

$$h_{sic2}(t) = -h_{chnl2}(t) \quad (14)$$

In other words, if the phases of the coupled and filtered SIC signal are 180° out-of-phase, destructive interference is achieved, leading to signal cancellation. Further reduction of SI can be achieved using a 180° degree hybrid coupler. At the output of the hybrid coupler, the total coupled signal cancels out. As such, $y_1(t)$ and $y_2(t)$ are combined out of phase, leading to additional cancellation. In other words,

$$y_1(t) + y_2(t) = 0 \quad (15)$$

V. SELF-INTERFERENCE CANCELLATION CIRCUIT

In this section, we present the design and optimization of the SIC circuit. For our design, a 6-tap FIR-resonator is considered, as depicted in Fig. 8. The delay lines, attenuators, and resonator stub were optimized to achieve a filter response that satisfied (13) and (14). In other words, the hybrid FIR-resonator response can be matched conjugately to antenna channel response by adjusting the gain delay of the attenuators and the transmission lines (copper trace), respectively, across the desired frequency band (1-1.5 GHz). Adding resonator provides for additional tunable parameters and hence, extra degree of freedom to mimic the SI signal. We note that, in our SIC circuit design, we considered the measured results of the symmetric coupling of the fabricated 3-element antenna prototype, shown in Fig. 5 and Fig. 7.

For the three-element monopole array, one antenna acts as a Tx antenna and the other two antennas are Rx antennas (Rx1, Rx2). The coupling from Tx to Rx1 is denoted as $S(1,2)$, and coupling from Tx to Rx2 is denoted as $S(3,2)$. Let the signal transmitted from antenna 2 be $\widetilde{s}_2(t)$, hence the SI signal is at antenna Rx1 due to coupling is $\widetilde{s}_2(t)S(1,2)$. Similarly, the SI at Rx2 due to Tx is $\widetilde{s}_2(t)S(3,2)$. The coupling function can be expressed as $S(1,2)=S(3,2)=\frac{e^{-sT}}{(\alpha(s))}$ with $T=\frac{d}{c}$, where d is the inter-antenna distance, α is the attenuation constant. Here SI can be suppressed using SIC circuit (*viz.* FIR resonator) having transfer function (TF) $h_{sic}(t)=S(1,2)=S(3,2)$.

From the basic network, we know that the passive multiport networks corresponding to the antenna arrays with mutual coupling contain TFs with both zeros and poles in their integer-order polynomial representations. The approximation of such coupling functions using FIR resonator is possible. However, the only trade-off is the order of the FIR resonator. Here, we are using microstrip substrate to keep the circuit low profile. To reproduce this network's unit impulse response, an FIR filter would need to sample it at close intervals of time and use the sampled values as weights (*viz.* taps) for the FIR realization.

The TF of the FIR resonator can be represented using circuit taps and a resonator. The FIR resonator designed is static. Circuit taps are implemented using tap delay lines and tap coefficients. Open stub line is used to design the resonator circuit. To realize the FIR resonator in analog domain, the tap delays and resonator are realized by microstrip line and tap coefficients are realized by attenuators. The width and length of the delay lines, attenuators, and resonator stub are optimized to achieve a transfer function that is conjugately matched to the channel transfer function between the Tx and Rx antennas. Adding resonator provides for additional tunable parameters and hence, extra degrees of freedom to mimic the SI signal.

More in detail, we design a 5^{th} order circuit (*viz.* 6 taps). This topology is passive, as it only consists of passive elements: delay lines, attenuators, and a resonator stub. The width and length of the delay lines, attenuators, and resonator stub are optimized to achieve a TF that is conjugately matched

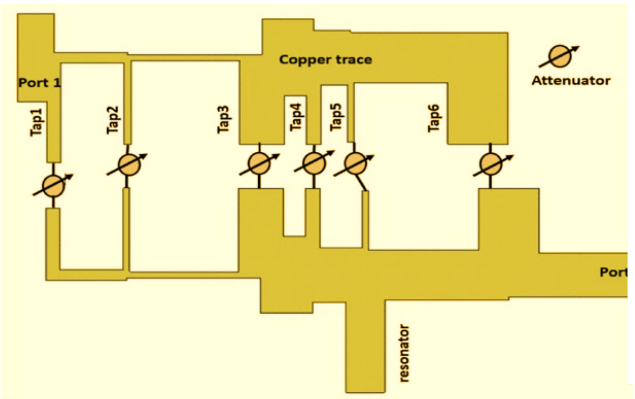

FIGURE 9. EM model of FIR- resonator circuit.

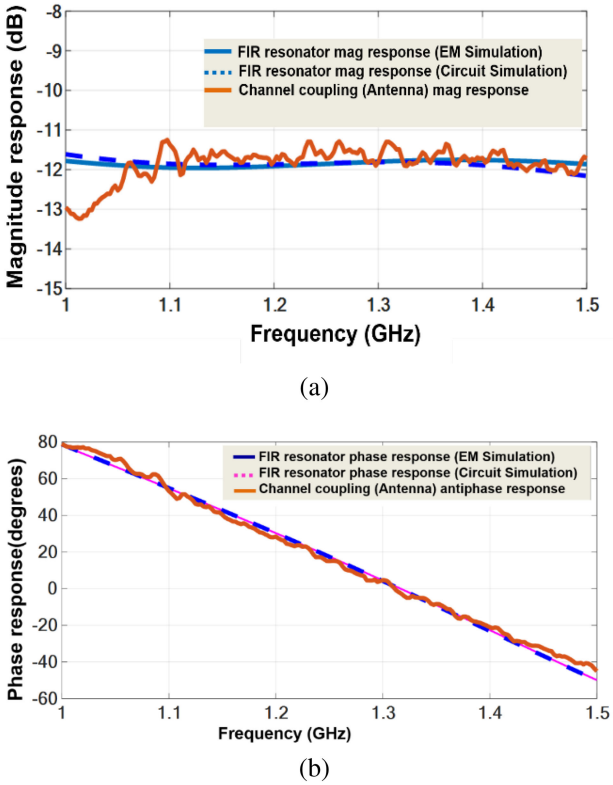

FIGURE 10. Simulation results showing the (a) magnitude and (b) phase response of the simulated hybrid FIR- resonator circuit, and the complex conjugate of the channel.

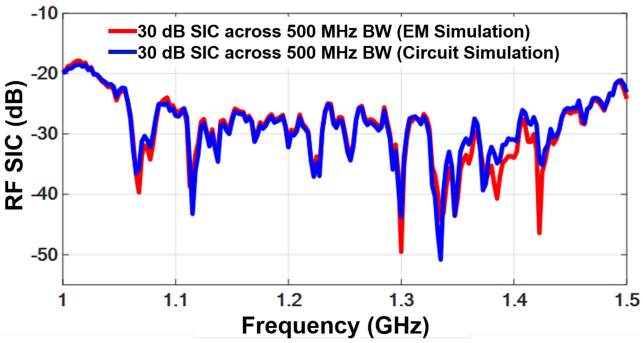

FIGURE 11. Computed SIC using the simulation results showing an average cancellation of ∼30 dB at each of Rx ports.

to the channel's TF (between the TX and Rx antennas). The delay spread and filter coefficients are obtained using a DE algorithm. For optimization, we have considered several factors. To calculate population size, a general rule is to multiply the number of optimizable parameters by 5 until the maximum number of parameters is reached (60 in this case). A small population size produces faster results, but it is also more likely to stall in a local optimum. Independent of the number of parameters, population sizes greater than 60 are generally not beneficial. In our circuit tuning for mimicking the coupling response, our population size was always less than 60. In our SIC design, we have chosen greedy strategy, since it produces the most rapid results. With no initial guess, the problem becomes complex. Therefore, we have chosen higher cross over probability. Typical values are between 0.0 and 1.0. In our case, the cross over probability is 0.9. We first performed circuit simulation to get the optimum weights of the circuit elements using this algorithm.

For fabrication purposes, circuit simulation is not enough to get the accurate result for SIC cancellation. Therefore, we have performed an EM simulation to get more accurate results. Here also, DE algorithm was also performed with the EM simulation. The EM model is developed, as shown in Fig. 9. We considered the vendor's actual S-parameter of the circuit element so that the fabricated prototype is well-matched to the antenna coupling. In brief, EM simulation of the circuit elements' actual S parameter helps find total optimum weights. The specific filter taps (*viz.* weighted filter) coefficient are 3, 3, 5, 0, 0, 15 and delay spread are 0.02, 0.039, 0.065, 0.015, 0.017, 0.063 ns at the center frequency. Insertion loss depends on the mutual coupling of the antenna array. The insertion loss of the FIR resonator is defined by $-20log_{10}|S(2,1)|dB$ and is shown in Fig. 10(a). We note that, the dimension of the SIC circuit is 37 mm×31 mm. A comparison between the magnitude response and phase response of the FIR-resonator and complex conjugate of the channel is depicted in Fig. 10(a) and (b). Clearly, the magnitude and phase response of the FIR-resonator and the channel between Tx and Rx antennas are in good agreement across 500 MHz bandwidth. Then, using the FIR-resonator response, SIC is computed according to the following expression [3]:

$$SIC_{dB} = \left[20\log_{10}\frac{1}{2\mid h_{chnl,n}\mid^2}(\mid h_{chnl,n}\mid^2 + \mid h_{sic,n}\mid^2) + 2\mid h_{chnl,n}\mid\mid h_{sic,n}\mid\cos(< h_{sic,n} - < h_{chnl,n})\right]^2 \quad (16)$$

Using (16), an average of 30 dB suppression is obtained from 1 to 1.5 GHz, as also shown in Fig. 11.

Since we are building the SIC circuit across a wider frequency range, the variable delay lines provide greater flexibility in terms of achieving cancellation. A fixed delay line is

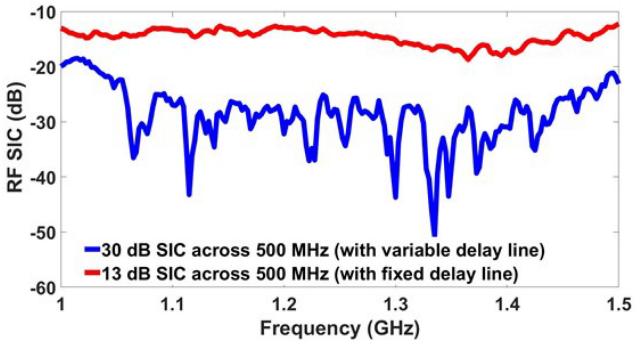

FIGURE 12. Effect of variable and fixed delay lines on SIC.

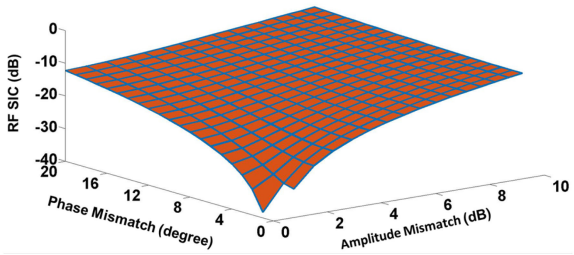

FIGURE 13. Effect of amplitude mismatch and phase mismatch on SIC.

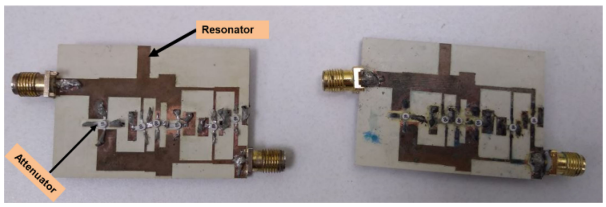

FIGURE 14. Fabricated RF FIR-resonator prototypes.

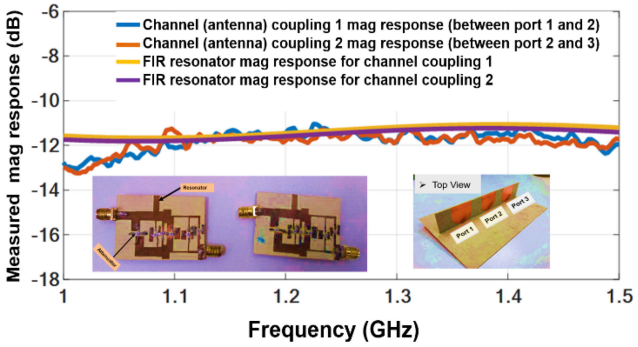

(a)

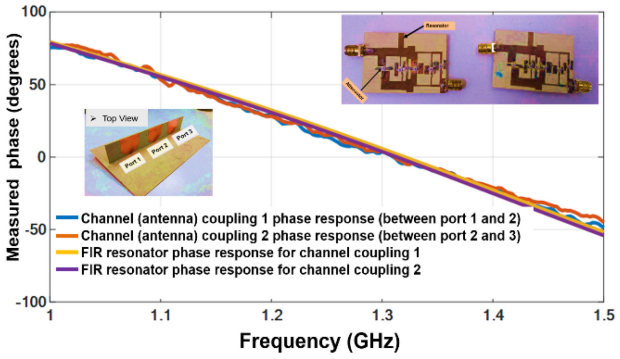

(b)

FIGURE 15. Measured results showing the (a) magnitude and (b) phase response of the fabricated hybrid FIR-resonator circuit, with the complex conjugate of the channel.

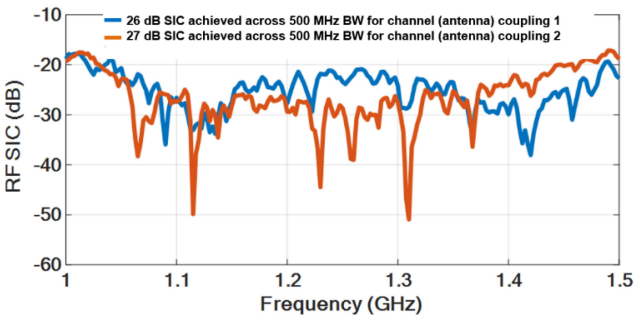

FIGURE 16. Computed SIC using the measured results showing an average of ∼26.5 dB cancellation at each of Rx ports.

also able to provide SI cancellation despite the fact that it is operating within a limited bandwidth. Fig. 12 shows the RF SIC response using SIC circuit for fixed and variable delay lines.

For STAR, amplitude and phase matching are critical factors in achieving the desired SI cancellation across operational bandwidth. We have commercial off-the-shelf (COTS) components in our system that contribute to phase and magnitude imbalance. The impact of phase and amplitude imbalances on the RFSIC is shown in Fig. 13.

VI. FABRICATED SELF-INTERFERENCE CANCELLATION CIRCUIT

Two FIR-resonator prototypes were fabricated for each of the symmetric channels, as shown in Fig. 14. Each prototype was constructed on TMM10 substrate with dielectric constant of 9.2, loss tangent of 0.0027, and substrate thickness of 1.52 mm. Fig. 15 show the measured magnitude and phase responses of the fabricated prototypes, demonstrating excellent matching with the antenna coupling responses. Using (16), these results imply 26 dB and 27 dB SIC of the coupled signal at each of Rx antenna, as depicted in Fig. 16. The slight discrepancy between the channel coupling and measured FIR resonator results are mainly due to fabrication tolerances.

VII. OVERALL RF SELF-INTERFERENCE CANCELLATION SYSTEM

Additional cancellation is achieved using a 180° hybrid coupler to combine the cancelled signals $y_1(t)$ and $y_2(t)$ at the

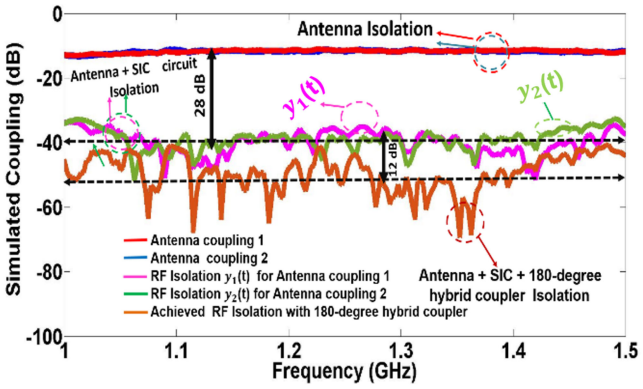

FIGURE 17. SIC of the simulated two-stage SIC system showing ~ 52 dB cancellation.

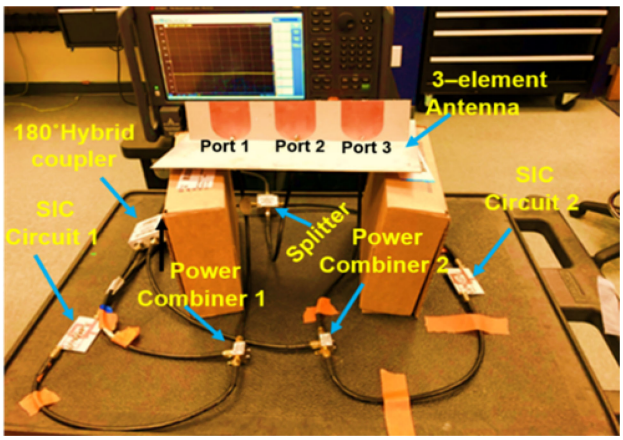

FIGURE 18. Measurement setup of the two-stage SIC system.

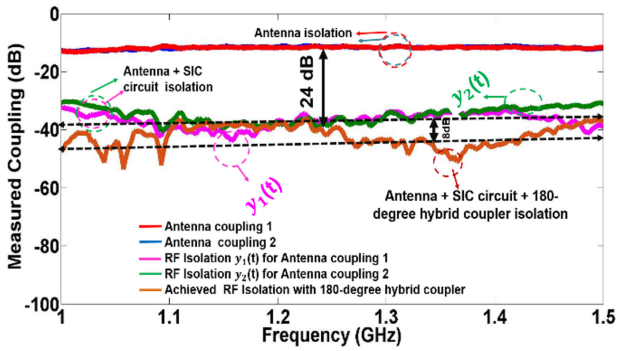

FIGURE 19. SIC of the measured two-stage SIC system showing ~44 dB cancellation.

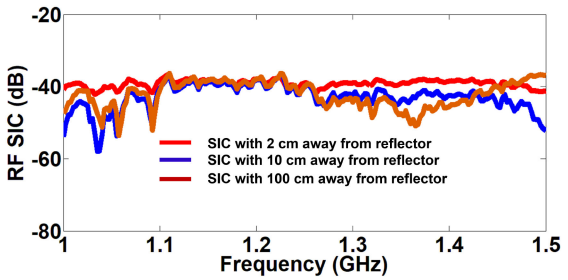

FIGURE 20. SIC performance with a reflector (antenna) placed at different distances.

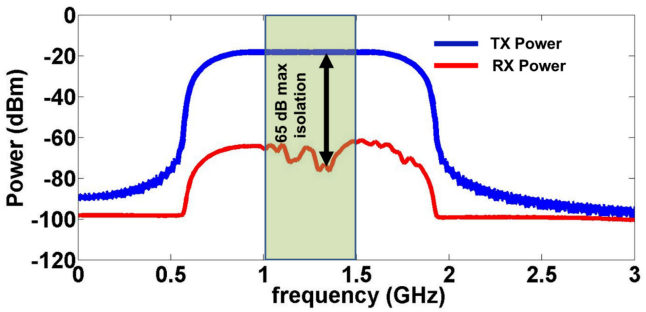

FIGURE 21. SIC with a QPSK signal. Simulated performance shows cancellation with a maximum of 65 dB and an average of 52 dB across the operational BW (1 to 1.5 GHz).

output of the power combiner at each of the Rx sides, as depicted in Fig. 1. Doing so, simulation shows that up to 65 dB with average 52 dB of coupling suppression across 500 MHz is achieved (see Fig. 17). Particularly, the addition of a hybrid coupler provides additional 12 dB avg. isolation between the Tx and combined Rx port, as depicted in Fig. 17.

To verify the simulation, we carried out a laboratory experiment using our combined RF analog cancellation topology. The measurement setup is depicted in Fig. 18. The system was not evaluated in isolated environment. It is worth mentioning that the accuracy of the measurements is contingent to the accuracy of the attenuators values, exact phase balance of each power combiner, and hybrid coupler losses. Fig. 19 shows an average measured cancellation of 44 dB with a minimum of 40 dB suppression across a BW of 500 MHz. In the measurements, the hybrid coupler provided an average of 8 dB of additional cancellation across 500 MHz. However, we note that an average of 11 dB cancellation was observed across 1.25 GHz to 1.45 GHz, implying a total of 47 dB average cancellation. We note that the insertion losses of the hybrid couplers and power combiners were subtracted from overall SIC in Fig. 17 and Fig. 19.

To evaluate the effect of reflections of neighboring objects, we have placed a reflector antenna at different distances away from our setup. In particular, the reflector was placed at 2 cm, 10 cm, and 100 cm. For each of these distances, measurements were conducted and SIC was computed, as shown in Fig. 20. It is obvious that SIC is not greatly affected by the position of the reflector. Undoubtedly, hardware non-idealities and calibration errors are the main cause of the slight difference between the simulated and measurement results.

We ran another experiment to test our STAR system with a modulated system. A Quadrature Phase Shift Keying (QPSK) modulated signal was generated and fed to the system with 0 dBm. Simulation results show an average isolation of 52 dB across a 500 MHz, as depicted in Fig. 21. The result was

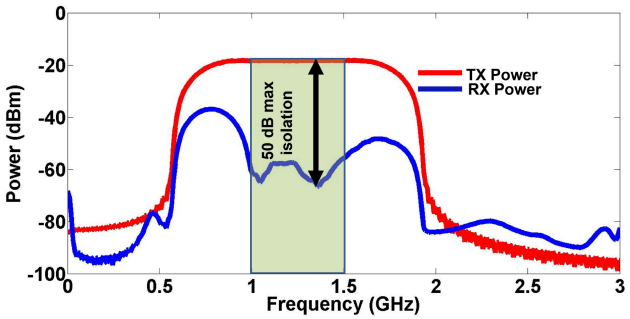

FIGURE 22. SIC with a QPSK signal. Measurements show cancellation with a maximum of 50 dB and an average of 44 dB across the operational BW (1 to 1.5 GHz).

also verified with our COTS components. An average SIC of 44 dB is achieved, which agrees with our simulated results. The measured performance is shown in Fig. 22.

VIII. COMPARISON WITH OTHER STATE-OF-ART STAR SYSTEM

In Table 1, we present a comparison of our 2-stage STAR implementation with other state-of-the-art systems. Early STAR architectures used two stages of interference cancellation: 1) antenna isolation and 2) analog post-processing to achieve up to 78 dB cancellation for very narrowband signals (20 MHz BW) [39]. Other bi-static STAR implementations achieved up to 60 dB cancellation across 80 MHz BW [34]. It is clearly shown that these techniques were all narrowband. On the contrary, research on wideband STAR has shown 25 dB to 50 dB (across $>$ 500 MHz), by only designing a single stage without a comprehensive system implementation [16], [46] or by introducing hardware complexity (*e.g.*, beamformer [44]). In our work, we implemented a two-stage wideband cancellation system based on the symmetric coupling cancellation technique with wideband cancellation. This is the first time a comprehensive two-stage STAR system is implemented using a low profile FIR resonator architecture. We have achieved an average of 52 dB (a minimum of 41 dB and a maximum of 65 dB) coupling cancellation across a BW of 500 MHz. Clearly, our design shows higher isolation for the wideband application with reduced hardware complexity.

IX. CONCLUSION

This paper presented a two-stage STAR architecture operating across 500 MHz that achieved 52 dB (a minimum of 41 dB and a maximum of 65 dB) coupling suppression between Tx and Rx ports. Our design consists of a three-element antenna (one Tx and two Rx) with a total isolation of 12 dB. Channel cancellation is achieved by implementing 6-tap FIR-resonator circuits between Tx and Rx antenna ports that increase the total isolation to 40 dB. The final stage consists of combining the two Rx ports using a 180° hybrid coupler to achieve overall average cancellation of 52 dB. Our system was fabricated and tested showing 44 dB (a minimum of 40 dB and a maximum of 50 dB) of measured cancellation. The discrepancy between simulation and measurement is mainly due to the fabrication tolerance, exact phase balance of the power combiner, hybrid coupler, and phase matched cables. This unprecedented wideband performance makes our STAR system a leading candidate for future 5 G communication.

REFERENCES

[1] L. Larson, "RF and microwave hardware challenges for future radio spectrum access," *Proc. IEEE*, vol. 102, no. 3, pp. 321–333, Mar. 2014.
[2] S. Hong *et al.*, "Applications of self-interference cancellation in 5G and beyond," *IEEE Commun. Mag.*, vol. 52, no. 2, pp. 114–121, Feb. 2014.
[3] S. B. Venkatakrishnan, E. A. Alwan, and J. L. Volakis, "Wideband RF self-interference cancellation circuit for phased array simultaneous transmit and receive systems," *IEEE Access*, vol. 6, pp. 3425–3432, 2018.
[4] S. K. Sharma, T. E. Bogale, L. B. Le, S. Chatzinotas, X. Wang, and B. Ottersten, "Dynamic spectrum sharing in 5G wireless networks with full-duplex technology: Recent advances and research challenges," *IEEE Commun. Surv. Tut.*, vol. 20, no. 1, pp. 674–707, Jan.–Mar. 2018.
[5] G. Liu, F. R. Yu, H. Ji, V. C. Leung, and X. Li, "In-band full-duplex relaying: A survey, research issues and challenges," *IEEE Commun. Surv. Tut.*, vol. 17, no. 2, pp. 500–524, Apr.–Jun. 2015.
[6] N. V. Shende, Ö. Güurbüz, and E. Erkip, "Half-duplex or full-duplex communications: Degrees of freedom analysis under self-interference," *IEEE Trans. Wireless Commun.*, vol. 17, no. 2, pp. 1081–1093, Feb. 2018.
[7] S. J. Watt, E. A. Alwan, W. Khalil, and J. L. Volakis, "Wideband self-interference cancellation filter for simultaneous transmit and receive systems," in *Proc. IEEE Int. Symp. Antennas Propag. USNC/URSI Nat. Radio Sci. Meeting*, Vancouver, BC, Canada, 2015, pp. 129–130.
[8] E. F. Alexanderson, "Simultaneous sending and receiving," *Proc. Inst. Radio Eng.*, vol. 7, no. 4, pp. 363–378, 1919.
[9] A. Hovsepian, E. A. Alwan, and J. L. Volakis, "A wideband, scanning array of four-arm spiral elements for simultaneous transmit and receive," *IEEE Antennas Wireless Propag. Lett.*, vol. 19, no. 4, pp. 537–541, Apr. 2020.
[10] A. Hovsepian, S. B. Venkatakrishnan, E. A. Alwan, and J. L. Volakis, "Wideband, scanning array for simultaneous transmit and receive," in *Proc. IEEE Int. Appl. Comput. Electromagn. Soc. Symp.*, Denver, CO, USA, 2018, pp. 1–2.
[11] E. A. Etellisi, M. A. Elmansouri, and D. S. Filipovic, "Wideband dual-mode monostatic simultaneous transmit and receive antenna system," in *Proc. IEEE Int. Symp. Antennas Propag.*, Fajardo, Puerto Rico, 2016, pp. 1821–1822.
[12] H. C. Papadopoulos and C.-E. Sundberg, "Reduction of mixed cochannel interference in microcellular shared time-division duplexing (STDD) systems," *IEEE Trans. Veh. Technol.*, vol. 47, no. 3, pp. 842–855, Aug. 1998.
[13] L. Dong, "Open-loop beamforming for frequency-division duplex mobile wireless access," *IEEE Trans. Veh. Technol.*, vol. 56, no. 4, pp. 1845–1849, Jul. 2007.
[14] R. Esmailzadeh, M. Nakagawa, and E. A. Sourour, "Time-division duplex CDMA communications," *IEEE Pers. Commun.*, vol. 4, no. 2, pp. 51–56, Apr. 1997.
[15] H. Holma, S. Heikkinen, O.-A. Lehtinen, and A. Toskala, "Interference considerations for the time division duplex mode of the UMTS terrestrial radio access," *IEEE J. Sel. Areas Commun.*, vol. 18, no. 8, pp. 1386–1393, Aug. 2000.
[16] S. Bojja-Venkatakrishnan, E. A. Alwan, and J. L. Volakis, "Wideband RF and analog self-interference cancellation filter for simultaneous transmit and receive system," in *Proc. IEEE Int. Symp. Antennas Propag. USNC/URSI Nat. Radio Sci. Meeting*, San Diego, CA, USA, 2017, pp. 933–934.
[17] A. Sabharwal, P. Schniter, D. Guo, D. W. Bliss, S. Rangarajan, and R. Wichman, "In-band full-duplex wireless: Challenges and opportunities," *IEEE J. Sel. Areas Commun.*, vol. 32, no. 9, pp. 1637–1652, Sep. 2014, doi: 10.1109/JSAC.2014.2330193.
[18] R. Lian, T.-Y. Shih, Y. Yin, and N. Behdad, "A high-isolation, ultra-wideband simultaneous transmit and receive antenna with monopole-like radiation characteristics," *IEEE Trans. Antennas Propag.*, vol. 66, no. 2, pp. 1002–1007, Feb. 2018.

[19] D. Bharadia, E. McMilin, and S. Katti, "Full duplex radios," in *Proc. ACM SIGCOMM Conf. Comput. Commun. Rev.*, Hong Kong, China 2013, pp. 375–386.

[20] A. Hovsepian, S. B. Venkatakrishnan, E. A. Alwan, and J. L. Volakis, "Wideband beam steering using a 4-arm spiral array for simultaneous transmit and receive (STAR) operation," in *Proc. IEEE Int. Symp. Antennas Propag. USNC/URSI Nat. Radio Sci. Meeting*, Boston, MA, USA, 2018, pp. 1915–1916.

[21] E. A. Alwan, A. Hovsepian, and J. L. Volakis, "Ultra-wideband dual polarization arrays with collocated elements for high isolation simultaneous transmit and receive systems," in *Proc. IEEE Int. Symp. Phased Array Syst. Technol.*, Waltham, MA, USA, 2016, pp. 1–3.

[22] A. Hovsepian, E. A. Alwan, and J. L. Volakis, "Wideband scanning array of spiral antennas for simultaneous transmit and receive (STAR)," in *Proc. IEEE Int. Symp. Antennas Propag. USNC/URSI Nat. Radio Sci. Meeting*, San Diego, CA, USA, 2017, pp. 487–488.

[23] K. E. Kolodziej, B. T. Perry, and J. S. Herd, "In-band full-duplex technology: Techniques and systems survey," *IEEE Trans. Microw. Theory Techn.*, vol. 67, no. 7, pp. 3025–3041, Jul. 2019, doi: 10.1109/TMTT.2019.2896561.

[24] D. Carsenat and C. Decroze, "UWB Antennas beamforming using passive time-reversal device," *IEEE Antennas Wireless Propag. Lett.*, vol. 11, pp. 779–782, 2012.

[25] H. Liu, S. Gao, and T. H. Loh, "Compact dual-band antenna with electronic beam-steering and beamforming capability," *IEEE Antennas Wireless Propag. Lett.*, vol. 10, pp. 1349–1352, 2011.

[26] W. Wei, W. Jing, L. Aimeng, and G. Meng, "Design of 2 by 2 dual-polarized antenna array with high isolation, wideband and low cross polarization," in *Proc. IEEE Int. Symp. Antennas Propag. USNC/URSI Nat. Radio Sci. Meeting*, San Diego, CA, USA, 2017, pp. 2161–2162.

[27] Y.-M. Zhang and J.-L. Li, "Differential-series-fed dual-polarized traveling-wave array for full-duplex applications," *IEEE Trans. Antennas Propag.*, vol. 68, no. 5, pp. 4097–4102, May 2020.

[28] K. L. Scherer *et al.*, "Simultaneous transmit and receive system architecture with four stages of cancellation," in *Proc. IEEE Int. Symp. Antennas Propag. USNC/URSI Nat. Radio Sci. Meeting*, Vancouver, BC, Canada, 2015, pp. 520–521.

[29] S. J. Watt, E. A. Alwan, and J. L. Volakis, "Cascaded network analysis of a wideband RF self-interference cancellation (RF-SIC) filter for STAR systems," in *Proc. IEEE Int. Symp. Antennas Propag.*, Fajardo, Puerto Rico, 2016, pp. 2117–2118.

[30] A. V. Oppenheim, *Discrete-Time Signal Processing*. Noida, India: Pearson Educ., 1999.

[31] N. Ginzberg, D. Regev, G. Tsodik, S. Shilo, D. Ezri, and E. Cohen, "A full-duplex quadrature balanced RF front end with digital pre-PA self-interference cancellation," *IEEE Trans. Microw. Theory Techn.*, vol. 67, no. 12, pp. 5257–5267, Dec. 2019.

[32] G. Karawas, K. Goverdhanam, and J. Koh, "Wideband active interference cancellation techniques for military applications," in *Proc. 5th Eur. Conf. Antennas Propag.*, Rome, Italy, 2011, pp. 390–392.

[33] M. Duarte and A. Sabharwal, "Full-duplex wireless communications using off-the-shelf radios: Feasibility and first results," in *Proc. Conf. Rec. 44th Asilomar Conf. Signals, Syst, Comput.*, Pacific Grove, CA, USA, 2010, pp. 1558–1562.

[34] D. Lee and B.-W. Min, "1-TX and 2-RX in-band full-duplex radio front-end with 60 dB self-interference cancellation," in *Proc. IEEE MTT-S Int. Microw. Symp.*, Phoenix, AZ, USA, 2015, pp. 1–4.

[35] A. T. Wegener, "Broadband near-field filters for simultaneous transmit and receive in a small two-dimensional array," in *Proc. IEEE MTT-S Int. Microw. Symp.*, Tampa, FL, USA, 2014, pp. 1–3.

[36] J. Zhou, T.-H. Chuang, T. Dinc, and H. Krishnaswamy, "Integrated wideband self-interference cancellation in the RF domain for FDD and full-duplex wireless," *IEEE J. Solid-State Circuits*, vol. 50, no. 12, pp. 3015–3031, Dec. 2015.

[37] K.-D. Chu, M. Katanbaf, T. Zhang, C. Su, and J. C. Rudell, "A broadband and deep-TX self-interference cancellation technique for full-duplex and frequency-domain-duplex transceiver applications," in *Proc. IEEE Int. Solid-State Circuits Conf.*, San Francisco, CA, USA, 2018, pp. 170–172.

[38] A. Nagulu *et al.*, "A full-duplex receiver with true-time-delay cancelers based on switched-capacitor-networks operating beyond the delay–bandwidth limit," *IEEE J. Solid-State Circuits*, vol. 56, no. 5, pp. 1398–1411, May 2021.

[39] K. E. Kolodziej, J. G. McMichael, and B. T. Perry, "Multitap RF canceller for in-band full-duplex wireless communications," *IEEE Transactions Wireless Commun.*, vol. 15, no. 6, pp. 4321–4334, Jun. 2016.

[40] W.-E. Kassa, A.-L. Billabert, S. Faci, and C. Algani, "Electrical modeling of semiconductor laser diode for heterodyne RoF system simulation," *IEEE J. Quantum Electron.*, vol. 49, no. 10, pp. 894–900, Oct. 2013.

[41] J. I. Choi, M. Jain, K. Srinivasan, P. Levis, and S. Katti, "Achieving single channel, full duplex wireless communication," in *Proc. 16th Annu. Int. Conf. Mobile Comput. Netw.*, Chicago, IL, USA, 2010, pp. 1–12.

[42] M. Jain *et al.*, "Practical, real-time, full duplex wireless," in *Proc. 17th Annu. Int. Conf. Mobile Comput. Netw.*, Las Vegas, NV, USA, 2011, pp. 301–312.

[43] E. A. Etellisi, M. A. Elmansouri, and D. S. Filipovic, "Wideband monostatic simultaneous transmit and receive (STAR) antenna," *IEEE Trans. Antennas Propag.*, vol. 64, no. 1, pp. 6–15, Jan. 2016.

[44] K. Kolodziej, P. Hurst, A. Fenn, and L. Parad, "Ring array antenna with optimized beamformer for simultaneous transmit and receive," in *Proc. IEEE Int. Symp. Antennas Propag.*, Chicago, IL, USA, 2012, pp. 1–2.

[45] S. B. Venkatakrishnan, A. Hovsepian, E. A. Alwan, and J. L. Volakis, "RF cancellation of coupled transmit signal and noise in STAR across 1 GHz bandwidth," in *Proc. URSI Int. Symp. Electro Magn. Theory*, San Diego, CA, USA, 2019, pp. 1–4.

[46] S. Bojja-Venkatakrishnan, E. A. Alwan, and J. L. Volakis, "Simultaneous transmit and receive system with 1 GHz RF cancellation bandwidth," in *Proc. IEEE Int. Symp. Antennas Propag. USNC/URSI Nat. Radio Sci. Meeting*, Boston, MA, USA, 2018, pp. 1241–1242.

[47] M. N. A. Tarek, M. Novak, and E. A. Alwan, "RF coupling suppression circuit for simultaneous transmit and receive systems," in *Proc. IEEE Int. Symp. Antennas Propag. North Amer. Radio Sci. Meeting*, Montréal, QC, Canada, 2020, pp. 1833–1834.

[48] S. M. Sohn, J. T. Vaughan, R. L. Lagore, M. Garwood, and D. Idiyatullin, "*In vivo* MR imaging with simultaneous RF transmission and reception," *Magn. Reson. Med.* vol. 76, no. 6, pp. 1932–1938, 2016, doi: 10.1002/mrm.26464.

MD NURUL ANWAR TAREK (Graduate Student Member, IEEE) received the B.E. degree in electrical and electronics engineering from the Chittagong University of Engineering and Technology, Chittagong, Bangladesh, in 2013, and the M.E. degree from Georgia Southern University, Statesboro, GA, USA. He is currently working toward the Ph.D. degree with Florida International University, Miami, FL, USA. He is also a Research Assistant with Smartmillimeter Wave RF Technologies (SmARTech) Lab, Florida International University, Miami, FL, USA. His research interests include full-duplex for 5G communication systems, millimeter wave-mixers, RF front ends, and implant antennas for medicinal purposes.

RIMON HOKAYEM (Member, IEEE) received the M.E. degree in electrical and computer engineering from the Lebanese University–Faculty of Engineering II, Roumieh, Lebanon, in 2014, and the Ph.D. degree in electrical and computer engineering from Florida International University, Miami, FL, USA, in 2021. He completed the M.E. thesis on field-programmable gate array (FPGA) programming for data acquisition and processing of gamma-rays during his internship with the Centre de Sciences Nucléaires et de Sciences de la Matiéreé (CSNSM/IN2P3/CNRS), Ile-de-France, France, in 2014. His research interests include radio frequency systems with an emphasis on beamforming and system design, from 2018 to 2021.

SANDHIYA REDDY GOVINDARAJULU (Student Member, IEEE) received the B.E. degree in electronics and communication engineering and the M.E. degree in communication systems from Anna University, Chennai, India, in 2013 and 2015, respectively. She is currently working toward the Ph.D. degree with Florida International University, Miami, FL, USA. During the master's degree studies, she was an Intern Researcher with the Society for Applied Microwave Electronics Engineering and Research, India. She was a Program Analyst with Cognizant Technology Solutions, Chennai, India. Her research interests include millimeter-wave antennas for 5G communication systems, beamforming, and RF front end. She was the recipient of the Best Student Paper Award for her research work at iWAT 2019.

MARKUS H. NOVAK (Member, IEEE) received the B.Sc. degree *(summa cum laude)* in electrical and computer engineering and the M.Sc. and Ph.D. degrees from The Ohio State University, Columbus, OH, USA, in 2013, 2016, and 2017, respectively. He has placed in two international best paper competitions and an International NASA Design Challenge. He was a Research Assistant with the Air Force Institute of Technology, Wright-Patterson AFB, OH, USA, a Product Engineer with Texas Instruments, Dallas, TX, USA, and a Research Fellow with the ElectroScience Laboratory, The Ohio State University. From 2017 to 2018, he was a Postdoctoral Researcher with Florida International University, Miami, FL, USA. Since 2018, he has been the President of Novaa Ltd., Chicago, IL, USA, where he leads research in wireless sensing and communications technologies for telecom, aerospace, and defense applications. He was PI on over a dozen commercial and Defense contracts. He has coauthored the Ultra-wideband arrays chapters of both *Antenna Engineering Handbook*, 5th edition (McGraw-Hill) and *Developments in Antenna Analysis and Synthesis* (Institution of Engineering and Technology), and more than 15 journal and conference papers. He holds several pending patents. His current research interests include ultra-wideband antennas, millimeter-wave systems, and low-cost beamforming architectures. He was the recipient of the NASA Space Technology Research Fellowship from 2013 to 2017.

ELIAS A. ALWAN (Member, IEEE) was born in Aitou, Lebanon, in 1984. He received the B.E. degree *(summa cum laude)* in computer and communication engineering from Notre Dame University–Louaize, Zouk Mosbeh, Lebanon, in 2007, the M.E. degree in electrical engineering from the American University of Beirut, Beirut, Lebanon, in 2009, and the Ph.D. degree in electrical and computer engineering from The Ohio State University (OSU), Columbus, OH, USA, in 2014. He is currently an Eminent Scholar Chaired Assistant Professor with the Department of Electrical and Computer Engineering, Florida International University, Miami, FL, USA. From 2015 to 2017, he was a Senior Research Associate with the Electro Science Laboratory, OSU. His research interests include antennas and radio frequency systems with particular focus on ultra-wideband communication systems, including UWB arrays, reduced hardware and power-efficient communication back-ends, and millimeter-wave technologies for 5G applications. He was the recipient of the 2020 NSF CAREER Award. He has been a Phi Kappa Phi Member since 2010.